Eur J Nucl Med Mol Imaging (2017) 44:838–849
DOI 10.1007/s00259-016-3569-0

ORIGINAL ARTICLE

Healthy brain ageing assessed with 18F-FDG PET and age-dependent recovery factors after partial volume effect correction

Stijn Bonte[1,2,3] · Pieter Vandemaele[3] · Stijn Verleden[4] · Kurt Audenaert[4] · Karel Deblaere[3] · Ingeborg Goethals[3] · Roel Van Holen[2]

Received: 7 July 2016 / Accepted: 3 November 2016 / Published online: 23 November 2016

Abstract

Context and purpose The mechanisms of ageing of the healthy brain are not entirely clarified to date. In recent years several authors have tried to elucidate this topic by using ^{18}F-FDG positron emission tomography. However, when correcting for partial volume effects (PVE), divergent results were reported. Therefore, it is necessary to evaluate these methods in the presence of atrophy due to ageing. In this paper we first evaluate the performance of two PVE correction techniques with a phantom study: the Rousset method and iterative deconvolution. We show that the ability of the latter method to recover the true activity in a small region decreases with increasing age due to brain atrophy. Next, we have calculated age-dependent recovery factors to correct for this incomplete recovery. These factors were applied to PVE-corrected ^{18}F-FDG PET scans of healthy subjects for mapping the age-dependent metabolism in the brain.

Results Many regions in the brain show a reduced metabolism with ageing, especially in grey matter in the frontal and temporal lobe. An increased metabolism is found in grey matter of the cerebellum and thalamus.

Conclusion Our study resulted in age-dependent recovery factors which can be applied following standard PVE correction methods. Cancelling the effect of atrophy, we found regional changes in ^{18}F-FDG metabolism with ageing. A decreasing trend is found in the frontal and temporal lobe, whereas an increasing metabolism with ageing is observed in the thalamus and cerebellum.

Keywords Age · ^{18}F-FDG PET · Healthy subject · PVE correction

Electronic supplementary material The online version of this article (doi:10.1007/s00259-016-3569-0) contains supplementary material, which is available to authorized users.

✉ Stijn Bonte
StijnD.Bonte@UGent.be

1 IBiTech, Block B, entrance 36 De Pintelaan 185, B-9000 Ghent, Belgium

2 iMinds - Medical Image and Signal Processing (MEDISIP), Department of Electronics and Information Systems, Ghent University, Ghent, Belgium

3 Department of Radiology and Nuclear Medicine, University Hospital, Ghent, Belgium

4 Department of Psychiatry, University Hospital, Ghent, Belgium

Introduction

With the advent of positron emission tomography (PET) the brain metabolism can be mapped through detection of a glucose analogue radiotracer. This has proven to be a great tool in the expansion of our knowledge on brain function. However, the way in which the brain grows old is still not entirely unravelled by the scientific community. A thorough understanding of ageing is of great importance in the discrimination of the normal from the pathological brain.

In recent years several authors have investigated the influence of age on brain metabolism using fluorodeoxyglucose (^{18}F-FDG) PET in healthy subjects [1–12]. Most authors report a reduced metabolism in the ageing brain, especially in frontal regions. The decreased glucose uptake in some brain regions may reflect tissue loss or shrinkage (structural atrophy), decreased glucose metabolism, or both. It is known that for each sulcus the width and depth increases with increasing age [13] and that the ventricular spaces are relatively larger in older people [14]. This leads to an increasing amount of cerebrospinal fluid (CSF) surrounding the grey matter (GM). Moreover, the percentage GM within the brain decreases with age [15]. These developments influence the measurement of GM glucose metabolism due to the partial volume effect (PVE). This effect is caused by two distinct phenomena [16]: the 3-dimensional image blurring introduced by the finite spatial resolution of the imaging system and the tissue fraction effect caused by image sampling. The PVE affects primarily objects smaller than half the resolution of the scanner. Since the cerebral cortex has only a thickness of about 2-3mm, imaging of this structure with PET (resolution about 5mm) is particularly affected, especially if the cortical thickness is further reduced due to atrophy.

To correct for the decreased signal in the cortex caused by the PVE different methods exist based on a co-registered and segmented magnetic resonance imaging (MRI) scan [17–21]. When applying such a method to the analysis of age-related differences in brain metabolism, authors came to diverging conclusions. Some authors reported that all significant correlations between age and brain metabolism disappear after atrophy correction [22–24], while others observed a continuing trend of hypo-metabolism in the ageing brain [25–30]. These authors and others [1, 6, 9, 10] showed that the reduction in brain metabolism cannot be accounted for merely by atrophy.

Many researchers have investigated the performance of PVE correction techniques using a phantom study. However, evaluating these methods in realistic situations with various stages of atrophy has never been done. We can expect that the ability of a PVE correction method to recover the true activity decreases when a larger degree of atrophy is present. Therefore in this article we investigate this ability for two different PVE correction methods: the Rousset method (MRI-based) [31] and iterative deconvolution (PET-based) [32]. With a phantom study based on a large database of healthy subjects between the age of 19 and 76 years old, we search for region- and age-dependent recovery factors, which can be applied after PVE correction. Afterwards, we apply this method to the real ^{18}F-FDG PET scans and search for regional correlations between brain metabolism and age.

Materials and methods

Subjects

We studied 93 volunteers who were recruited in response to local advertisement in the hospital. We considered 82 among them to be healthy according to strict inclusion criteria as described below. They were between the age of 19 and 76 years old; the age distribution can be found in Table 1. All subjects are native Dutch-speaking. Regarding medication, oral contraceptives in pre-menopausal women and hormonal replacement therapy in postmenopausal women were allowed as well as oral medications for hypertension, hyperlipemia, diabetes, joint and back pain, and benign hypertrophy of the prostate. Individuals who were currently on psychotropic drugs were excluded as well as subjects with a personal history or current substance abuse.

Prior to the neuropsychological and the personality assessment, each healthy adult underwent a clinical neurological examination (by a senior neurologist) and a structured psychiatric interview (by a senior psychiatrist) to exclude (a history of) neurological and psychiatric disorders. Exclusion criteria based on the subject's medical history included central nervous disorders, such as a (possible) cerebrovascular accident, epilepsy, head trauma, dyslexia, migraine, and neurodegenerative disorders, and exclusion criteria based on the volunteers' psychiatric history included psychiatric disorders, such as mood and anxiety disorders and substance abuse. The neuropsychological assessment (by a clinical neuropsychologist) included a brief history to exclude subjective cognitive complaints (attention, executive functions, and memory functions) and to assess activities of the daily life. The aim of this assessment was to identify volunteers with evidence of behavioural and cognitive impairment. This method was preferred over the MMSE (mini-mental state examination [33]) because it is well known that the latter is less sensitive to detect cognitive dysfunction.

3-D magnetization-prepared rapid acquisition gradient echo (MPRAGE) brain MRI (without the administration of gadolinium) was performed to rule out anatomical brain abnormalities. In 31 subjects, MRI showed small to larger periventricular and deep white matter lesions that were attributable to normal ageing, judged by a senior neuroradiologist. Hence, these subjects were not excluded. Written

Table 1 Mean age and number of subjects per decade included in this study

	mean age±SD	18-29 years	30-39 years	40-49 years	50-59 years	60-69 years	70-79 years
men	50.0±16.2 years	7	6	5	8	13	4
women	44.2±16.5 years	10	6	6	8	7	2

informed consent was obtained from all subjects according the guidelines of the local medical ethics committee.

Imaging protocol

After the completion of the clinical examinations and cognitive testing, subjects underwent ^{18}F-FDG brain PET and MRI. The MRI examination was performed on a 3T Siemens Trio Tim System (Siemens, Erlangen, Germany) using a standard Siemens birdcage 8-channel head coil. A T1-weighted MPRAGE image was acquired in three orthogonal planes using the following parameters: TR = 1550ms, TE = 2.37ms, matrix size = 256 × 256 and 176 slices. This resulted in a volumetric image with an isotropic resolution of 0.9 × 0.9 × 0.9 mm^3.

^{18}F-FDG PET scans were performed on an Allegro PET imaging system (Philips Co., Cleveland, Ohio, USA), which consists of a gadolinium oxyorthosilicate (GSO) full-ring PET scanner with a spatial resolution of about 5mm (center FOV: 4.65mm vertical, 5.00mm horizontal FWHM; 10cm transverse offset Y: 5.47mm vertical, 5.25mm horizontal; 10cm transverse offset X: 5.26mm vertical, 5.66mm horizontal according to internal acceptance report). The system also includes caesium rods for transmission scanning. Prior to the PET scanning, subjects were instructed on how to sustain a mental state of Random Episodic Silent Thought (REST) during scanning, which means that they were instructed to lie quietly and relax and not perform any specific mental task. During this condition subjects think principally about past and future experiences [34]. Eyes were open, and ears were unplugged. Subjects lay comfortably on the scanner bed in a dimly lit room and ambient noise was kept to a minimum. Subjects fasted at least 4 hours before administration of the tracer to maintain serum glucose concentrations below 120mg/dL. First, a transmission scan of the skull was performed. This scan was used for attenuation correction purposes. Subsequently, after intravenous injection of 185MBq (5mCi) of ^{18}F-FDG and a distribution period of 30 minutes, a static emission scan of 15 minutes was acquired in high-resolution mode (matrix 128 × 128 × 90 and voxel size 2 × 2 × 2 mm^3). Reconstruction was performed using a 3-dimensional RAMLA (Row Action Maximum Likelihood) algorithm provided by the manufacturer [35] (blob radius 10mm, 8 subsets, 2 iterations). No post-filtering was performed. Scatter [36] and attenuation correction were applied. These reconstruction settings are the same as used in clinical practice and correspond to the parameters recommended by the manufacturer.

All original DICOM images are converted to NIfTI-1.1 format using MRIcron (available at www.mricro.com) and transferred to SPM12 (Wellcome Trust Centre for Neuroimaging, University College, London) running on MATLAB (version R2014b, MathWorks Inc., Natick, MA, USA). The PET image is co-registered with the T1-MRI scan of the same volunteer using the normalised mutual information method and resliced using a trilinear interpolation. All other parameters are kept to the default SPM12 settings. Next, the MRI scan is segmented into grey matter, white matter and CSF using the built-in segmentation tool. The MRI scan is now used to estimate the parameters for normalisation to the default template in MNI-space. A trilinear interpolation is used, all others settings are kept to default. The resulting images have 79 × 95 × 79 voxels with a voxel size of 2 × 2 × 2 mm^3.

Phantom study

PVE correction methods

To evaluate the performance of different partial volume effect correction methods, a phantom study is carried out. A schematic overview of this methodology is given in Fig. 1. After normalising the PET scan to MNI-space using SPM12, the original scan is corrected for the partial volume effect using two validated algorithms.

The first PVE correction technique (hereafter called MRI-PVE) is the Rousset method [31], an MRI-based algorithm. This method calculates the Geometric Transfer Matrix (GTM), which contains the amount of spill-in and spill-out of activity between different compartments. By inverting this matrix and multiplying it with the mean measured activity in each compartment, the original activity can be calculated. In this study the different compartments were defined by combining a brain atlas with the segmented MRI scan of each subject. First, a maximum probability brain atlas with 83 regions by Hammers et al. (2003) [37] is transformed to match the orientation and voxel size of the normalised PET scan using the SPM `imcalc` option. Next, for each subject these 83 regions are divided into grey matter, white matter and CSF using the corresponding segmented MRI tissues. The result is a subject-matched atlas with 250 regions (3 × 83 + background). Classes with 10 voxels or less are assigned to the largest neighbouring region, such that about 210-215 regions remain. These classes are used to calculate the GTM, with the assumptions of 5mm isotropic resolution.

The second method (hereafter called PET-PVE) is the iterative deconvolution using the Huber prior for denoising, as presented by B.A. Thomas [32]. This is a PET-based method where the image quality is iteratively improved by using knowledge of the resolution of the imaging system. We applied the approximation of a 5mm isotropic resolution and the following parameters: $\alpha = 0.2$, $\beta = 0.01$, $\gamma = 0.01$ and 500 iterations, as this ensured in the best possible extent the recovery of the true activity.

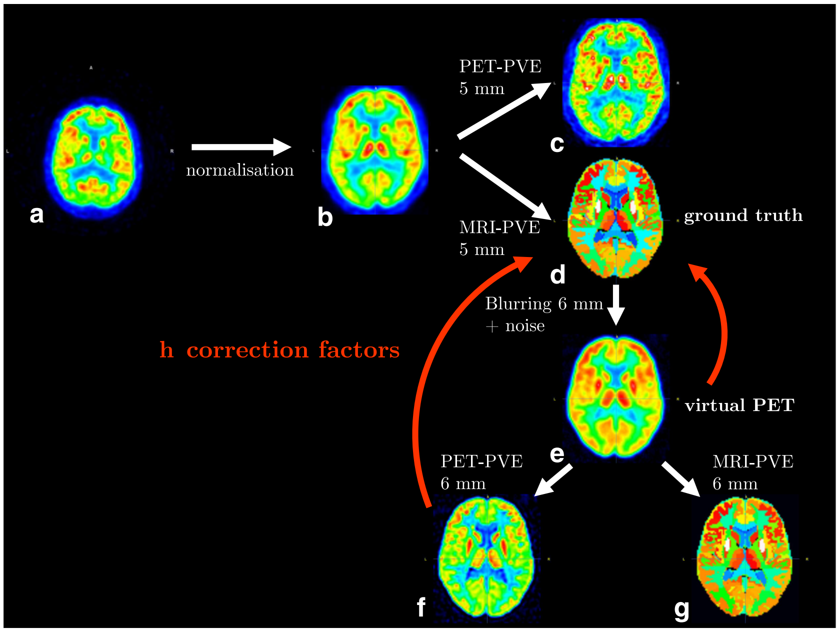

Fig. 1 Methodology of the study: **a** original PET scan; **b** normalised scan to MNI space using SPM12; **c** PVE corrected image using the iterative deconvolution method (PET-PVE) assuming an isotropic resolution of 5mm; **d** PVE corrected image using the Rousset method (MRI-PVE) assuming an isotropic resolution of 5mm, this image is considered the ground truth image for the phantom study; **e** virtual PET scan constructed by adding noise and 6mm Gaussian blurring to the ground truth scan; **f** PET-PVE corrected phantom image assuming an isotropic resolution of 6mm; **g** MRI-PVE corrected phantom image assuming an isotropic resolution of 6mm; **h** for each brain region, correction factors are calculated by dividing the mean intensity in the ground truth image by the mean intensity in the phantom images - this is done for the phantom PET image and both PVE corrected versions

Virtual PET data

For all patients, the image corrected with MRI-PVE is regarded as the ground truth image from which a virtual PET image is constructed. The Rousset correction is preferred as the ground truth, rather than a phantom with a constant activity in the GM and WM. This is necessary by acknowledging that in this way, with a realistic distribution of the activity, spill-in and spill-out between different brain region activities, also within the GM or WM, can be accounted for. The virtual PET image is constructed by first adding Gaussian noise with mean 0 and standard deviation equal to $1/20$ of the maximal intensity of the ground truth image. Next, 6mm isotropic gaussian blurring is applied, followed by again adding Gaussian noise with mean 0 and standard deviation equal to $1/200$ of the maximal intensity of the ground truth. This virtual PET image is again corrected with both PVE correction methods (6mm isotropic resolution).

Calculation of correction factors

The activity recovery in grey matter in the different brain regions of the Hammers atlas [37] is calculated as the mean activity in the virtual PET image and its PVE corrected versions divided by the activity in the ground truth scan. Recovery coefficients are plotted as a function of subject age for two different brain regions in Fig. 2. In each region of the atlas the offset β_0 and slope β_1 of the linear fit between the recovery coefficient and subject age are determined. For each subject and each brain region, an age-dependent correction factor is determined as $1/(\beta_0 + \beta_1 \times \text{age})$. When multiplying the mean activity in every region in the virtual PET scan and the PVE corrected versions with these correction factors, the logical result is that the mean recovery with age is put to one.

Application of age-dependent recovery factors to real PET scans

Now, the mean activity in the different grey matter regions of the real PET scans and their PVE corrected versions are multiplied with the age-dependent recovery factors $1/(\beta_0 + \beta_1 \times \text{age})$. Normalisation of the PET intensities is done by dividing the different grey matter activities by the mean intensity in the entire cerebellum after Rousset correction. Next, a linear regression between the normalised mean activity in the different grey matter regions and age is searched for. The correlation was considered significant when $p < 0.05$.

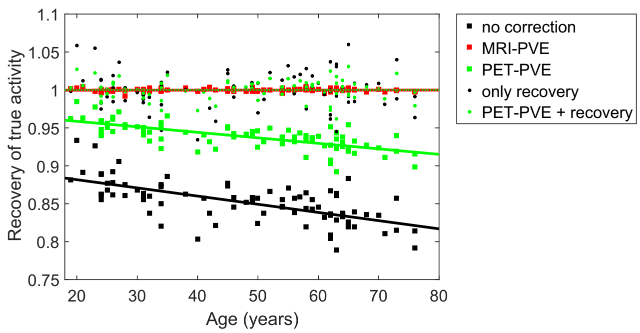

a Superior frontal gyrus right

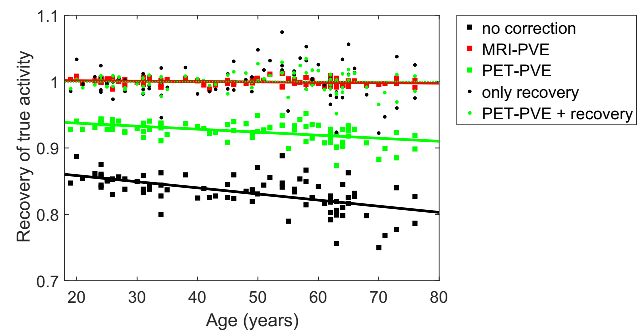

b Thalamus left

Fig. 2 Example of the activity recovery in two brain regions in the phantom study. The recovery (squares) is here defined as the mean intensity in the brain region divided by the ground truth intensity in this region. This is done for the virtual PET image and the PVE corrected versions. Age-dependent recovery coefficients are determined as $1/(\beta_0 + \beta_1 \times \text{age})$, where β_0 is the offset and β_1 the slope of the linear fit between recovery and age. This causes the mean corrected recovery over age to be equal to one (dots)

Results

Calculation of correction factors using virtual PET phantoms

The activity recovery, defined as the mean intensity in a certain brain region divided by the ground truth intensity in this region, is illustrated in Fig. 2 for two different regions: the right superior frontal gyrus and the left thalamus. For the MRI-PVE method, there is no significant influence of age on the recovery, which is one for all brain regions. The PET-PVE technique approaches the true activity better than without correction, but there remains a decreasing performance trend with increasing age. This explains the need for an age-dependent correction for this method. After multiplying the activity with the recovery factors, the expected activity recovery is one.

The recovery factors for the different grey matter brain regions are illustrated in Fig. 3 (see also Table 2 in the supplementary materials). Regions with a low percentage of grey matter, including brain stem, pallidum, corpus callosum, substantia nigra and the ventricles, are excluded from this list. Notice that recovery factors for the MRI-PVE method are unnecessary, since this technique already achieves a perfect recovery.

Application of correction factors to real PET scans

After application of the different PVE-methods to the real PET scans and multiplication with the recovery factors, in every region a linear relation between mean metabolism and age is investigated. An overview of the different significantly correlating grey matter regions with age is given in Table 2 in the supplementary materials. This is also illustrated in Fig. 5. Here the following measure of change in metabolism was chosen:

$$\Delta M = \frac{E[A_{76}] - E[A_{19}]}{E[A_{19}](76-19)} \times 100\,\% = \frac{\beta_1}{E[A_{19}]} \times 100\,\% \quad (1)$$

where $E[A_i]$ is the expected normalised activity in this region at age i and β_1 is the slope of the linear fit between the normalised activity and age. A positive ΔM means that there is an annual increase in metabolism with this percentage compared to the activity at age 19. A negative ΔM implies a decreasing metabolism with ageing. This is also illustrated for two brain regions in Fig. 4: in the right superior frontal gyrus a significant decreasing metabolism with age is observed, even after applying PVE and the recovery factors, whereas in the left thalamus a significant increasing metabolism is found.

As can be seen in Fig. 5 (and Table 2 in the supplementary materials) many regions show a decreasing metabolism with ageing, especially in the temporal and frontal lobes. An increase in ^{18}F-FDG uptake with age is seen in the cerebellum, the nucleus accumbens and thalamus. The original PET image and both the corrected versions largely show the same results, proving the robustness of our method.

Discussion

In literature, several authors have investigated the age-related differences in ^{18}F-FDG PET images. Most authors report a decreasing metabolism in the ageing brain, especially in frontal regions. However, when correcting for the partial volume effect, diverging results occurred. Some authors no longer observed significant changes and attributed the decreasing brain metabolism to atrophy. On the other hand, several authors proved that atrophy alone cannot explain the decreasing ^{18}F-FDG metabolism, since they observed a decreasing metabolism with age after correcting for atrophy. An overview of some recent studies

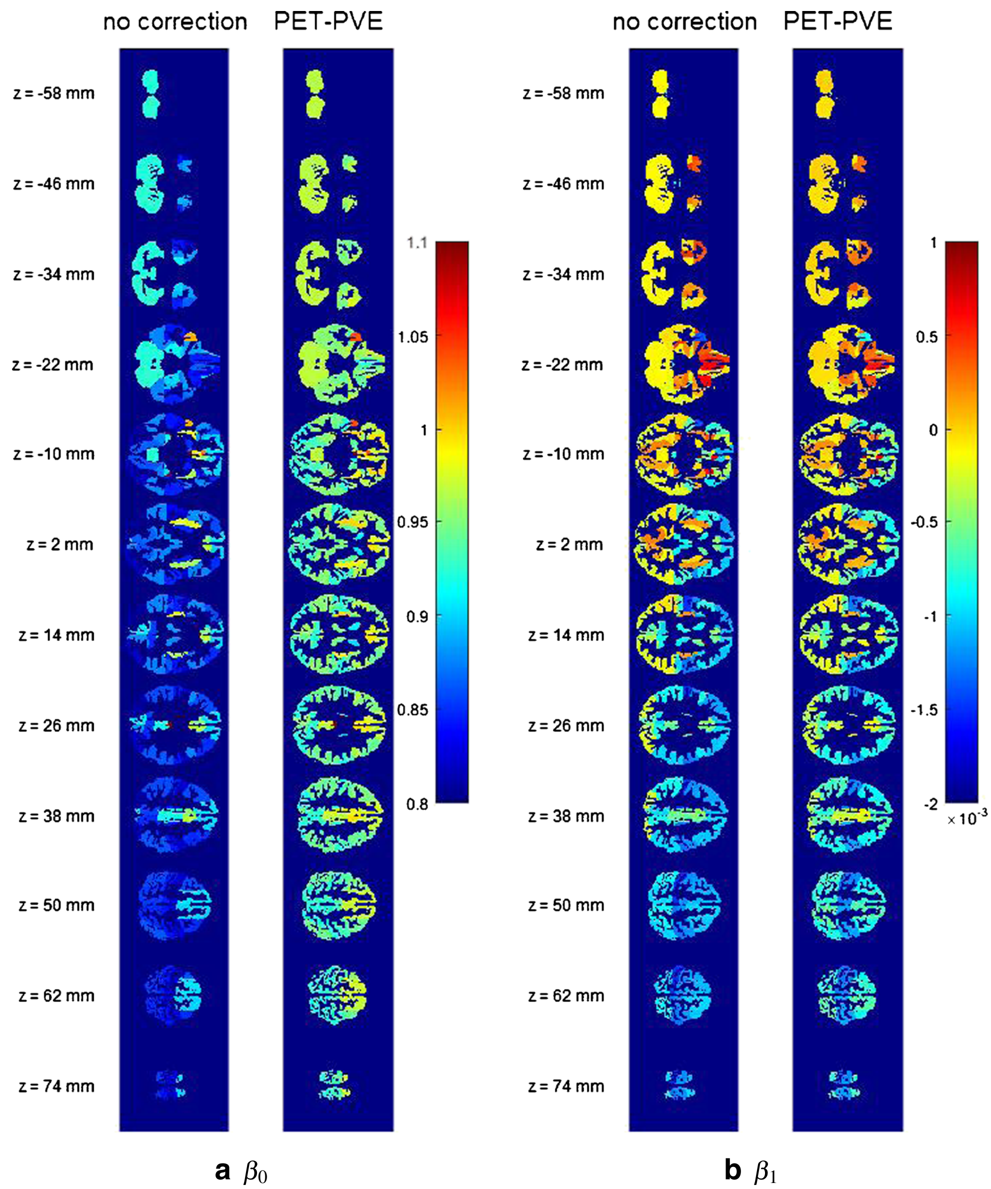

Fig. 3 Illustration of the recovery factors. To correct the mean uptake in a certain brain region, the activity should be divided by $\beta_0 + \beta_1 \times$ age. The colour scale is truncated for visual purposes. A list of values can also be found in the supplementary materials

using partial volume effect correction and corresponding results is given in Table 2.

No study so far has provided an age-dependent partial volume effect correction protocol. In this paper we have evaluated the performance of two validated methods at different ages using a phantom study. These methods are the Rousset technique (MRI-PVE) and iterative deconvolution (PET-PVE). When no partial volume effect correction is applied, the limited resolution of the imaging system restricts the ability to resolve small structures (see Fig. 2). This ability further decreases with decreasing structural dimensions. The PET-PVE method artificially improves the resolution post reconstruction, but this method is not able to achieve a perfect recovery. On the other hand, the MRI-PVE method is able to resolve the true activity in a region, regardless of the dimensions, which implies that the use of age-dependent recovery factors is redundant. This is however only true if a perfect mask of this region can be provided. With decreasing dimensions, it becomes harder for segmentation algorithms to obtain an accurate mask of the region to resolve. This is also due to the division of a scan in discrete voxels. The influence of different segmentation algorithms on the performance of MRI-based partial volume effect correction techniques has carefully been examined in literature [38–40].

In this study, we have applied a Region-of-Interest (ROI) study, consisting of the grey matter in several regions of a brain atlas. For each region, we have found age-dependent recovery factors which can be combined with the original PET image or the PET-PVE correction method. In this way

Table 2 Overview of recent studies investigating age-related differences in the healthy brain using ^{18}F-FDG PET after partial volume effect correction

author	**n**	method	PVE correction method	result
de Leon et al. [26] 2001	48 (60-80y)	ROI + SPM	Meltzer [18]	reduced metabolism with ageing in temporo-parietal cortex bilaterally and left inferior frontal gyrus
Ibáñez et al. [23] 2004	24 (22-34y; 55-82y)	SPM	Meltzer [18]	no significant correlation
Yanase et al. [27] 2005	139 (24-81y)	SPM	Matsuda [17]	reduced metabolism with ageing in bilateral anterior cingulate gyri, left precentral gyrus, bilateral inferior frontal gyri, left middle termporal gyrus, bilateral paracentral lobules
Kalpouzos et al. [25] 2009	45 (20-83y)	SPM	modified Müller-Gärtner [20]	reduced metabolism with ageing in bilateral superior medial frontal, motor, anterior and middle cingulate cortices, bilaterial parietal regions, superior temporal gyrus; less metabolic decrease in inferior temporal (fusiform cortex) and occipital areas
Kochunov et al. [24] 2009	19 (59-92y)	ROI	Park [21]	no significant correlation
Curiati et al. [22] 2010	58 (66-79y)	SPM	modified Müller-Gärtner [20]	no significant correlation
Knopmann et al. [28] 2014	806 (30-89y)	ROI	Meltzer [18]	reduced metabolism with ageing in putamen, insula, thalamus, anterior cingulate, supplementary motor, lateral temporal, caudate, orbital frontal, posterior cingulate and/or precuneus, frontal, rolandic operculum, lateral parietal, primary visual, precentral gyrus, occipital and medial temporal regions
Nugent et al. [29] 2014	44 (18-30y; 65-85y)	ROI + SPM	modified Müller-Gärtner [20]	reduced metabolism in older adults compared to young adults in superior frontal cortex, gyrus rectus, temporal cortex, anterior cingulate, insula, putamen and thalamus
Nugent et al. [30] 2014	56 (18-30y; 65-85y)	ROI	modified Müller-Gärtner [20]	reduced metabolism in older adults compared to young adults in superior frontal cortex, caudal middle frontal cortex and caudate nucleus
Current study 2016	82 (19-76y)	ROI	Rousset [31] and iterative deconvolution [32] (+ age-dependent recovery factors)	reduced metabolism with ageing in temporal lobe, frontal lobe, insula, cingulate gyrus, right lingual gyrus; increasing metabolism in cerebellum and thalamus

n = number of subjects; ROI = region of interest analysis; SPM = statistical parametric mapping

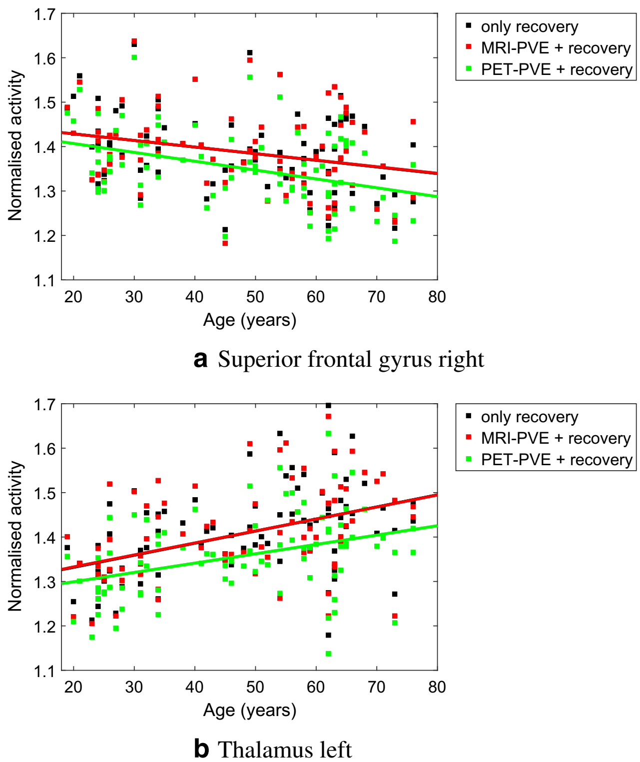

Fig. 4 Example of regions with a significant correlation between metabolism and age. The activities in grey matter are normalised to the mean intensity in the entire cerebellum

the correction is two-fold: first the PVE correction method corrects for atrophy, followed by an additional correction which takes into account the inability to perfectly recover the true activity from the cortex with a reduced thickness. Thus, a different correction is applied at different ages and there should be no remaining effect of atrophy in the results. For the MRI-PVE method, which is already able to perfectly recover the true activity, age-dependent recovery factors are not necessary.

Applying this method to ^{18}F-FDG PET scans of healthy subjects, we find a true decrease in metabolism with ageing in large parts of the brain (in 42 out of 83 brain regions), especially in the frontal and temporal lobe. This confirms the result of prior studies (cfr. Table 2). An increasing metabolism with age is found in the cerebellum, nucleus accumbens and thalamus. The increasing metabolism in the cerebellar grey matter is difficult to interpret because of the normalisation on the entire cerebellum. This means that the discovered increasing metabolism in the grey matter only reflects that the fraction of grey matter on the metabolism of the entire cerebellum increases with age. Moreover, the results in the nucleus accumbens should be interpreted with caution, because this is a very small region, which makes it very vulnerable to registration errors with the brain atlas.

The results show a remarkable agreement between the values for the PET-scan, the Rousset corrected version (MRI-PVE) and the PET-based correction by iterative deconvolution (PET-PVE) (cfr. Table 2 in the supplementary materials). There are eight brain regions (out of 83) where the different methods show a different behaviour of ΔM, the normalised change of metabolism with ageing, as can be seen in Table 2 of the supplementary materials. These five regions include the left parahippocampal and ambient gyri, the left posterior part of the superior temporal gyrus, the right anterior part of the superior temporal gyrus, the left middle frontal gyrus, the left subgenual frontal cortex, the right subcallosal area, the right inferiolateral remainder of the parietal lobe and the right nucleus accumbens. The different behaviour manifests itself mainly in the p-values. For these regions at least one method yields a p-value which is (often borderline) not significant, whereas other methods show a significant p-value. However, the general ΔM behaviour is closely related for all methods, as is clear in Fig. 5. This also means that the PET-PVE correction method can be safely used as an alternative for partial volume effect correction. Since with this method there are no assumptions on tracer distribution and there is no need for a perfectly coregistered MRI-scan, the technique can easily be implemented in a clinical and pathological setting. However, when applying the age-dependent recovery factors presented here, there is still a need for anatomical region masks.

If we compare the behaviour with ageing of atrophy and metabolism in our dataset, we observe similar trends in many brain areas. This is graphically depicted in Fig. 6. The slope and p-value are depicted here in different brain regions for both atrophy and the Rousset corrected metabolism. Atrophy is quantified as the cube root of the number of voxels within each grey matter region, which should be a good approximation of the cortical thickness. In regions with a limited amount of atrophy, such as the cerebellum, the occipital and parietal lobe, we observe little or positive changes in metabolism with ageing. In the orbitofrontal cortex we observe strong atrophy and also a profound decrease in metabolism. In the remainder of the frontal lobe, there is a lower amount of atrophy (yet very significant), but here we observe a strong decrease in metabolism with ageing. The most remarkable difference between atrophy and metabolism manifests itself in the central structures, where a large (yet insignificant) amount of atrophy is observed, but no or a positive trend in metabolism is shown. We want to stress that the metabolism in this picture is corrected for atrophy-related effects.

The suggested methodology can be applied in a broad spectrum of brain PET studies where an accurate quantification of the uptake is required. The recovery factors calculated in this study should only be applied to correct

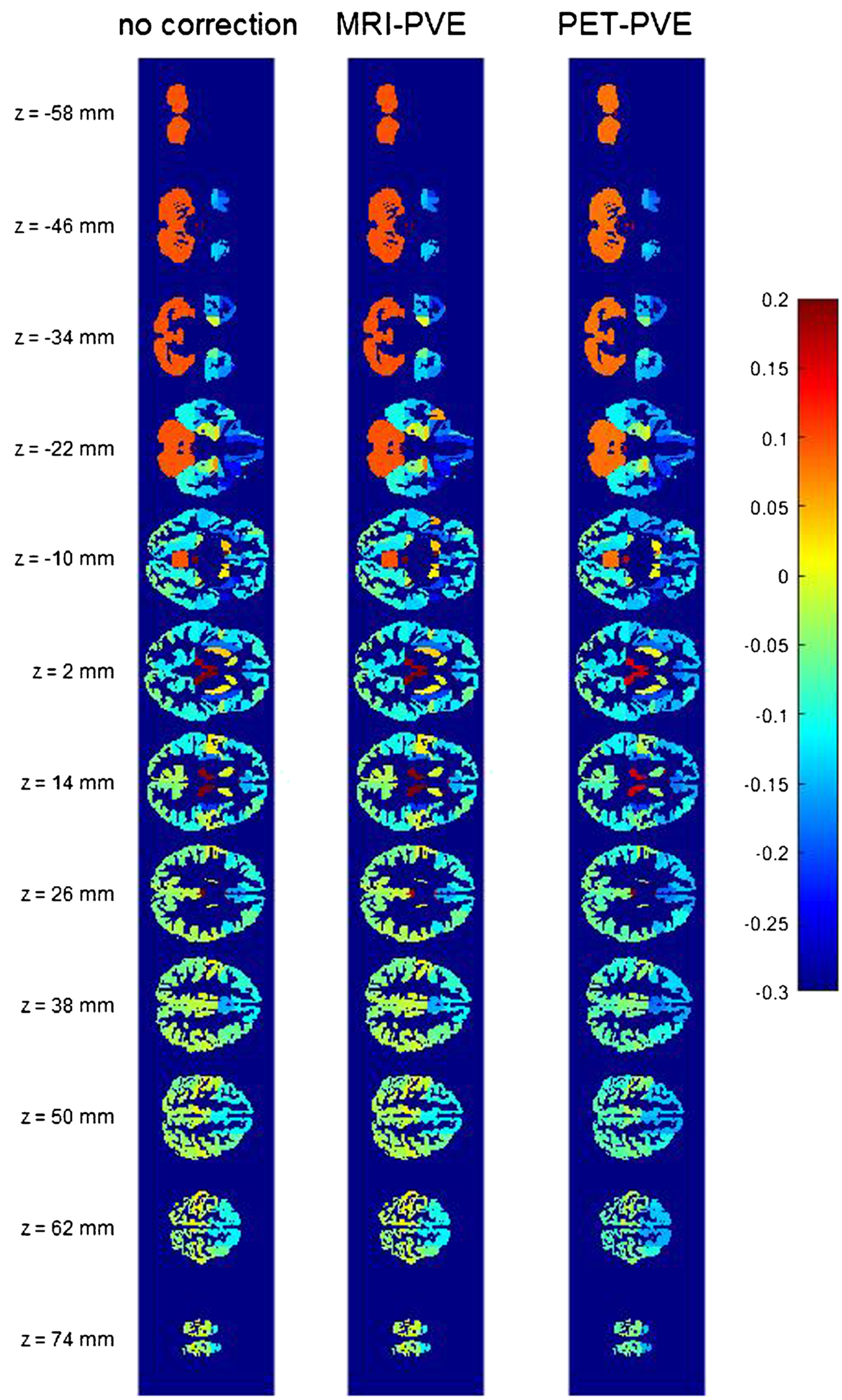

Fig. 5 Annual change of metabolism ΔM as defined in Eq. 1. The colour scale is truncated for visual purposes. A list of values can also be found in the supplementary materials

the uptake of healthy subjects. For other coherent populations, e.g. healthy subjects scanned using other radiotracers or early scanning time frames, one can consider to calculate a dedicated set of age-dependent recovery factors, as was done in this study. For a more heterogeneous population, e.g. when comparing pathological cases such as Alzheimer's disease to healthy controls, the use of individual (instead of population-based) recovery factors should be preferred. The methodology is the same as explained in "Phantom study" and Fig. 1: the uptake in different brain regions is estimated using the Rousset method, which is considered as the ground truth. A virtual PET-scan is constructed from this ground truth and, if desired, corrected for the partial volume effect. Comparing these scans to the ground truth yields the individual recovery factors.

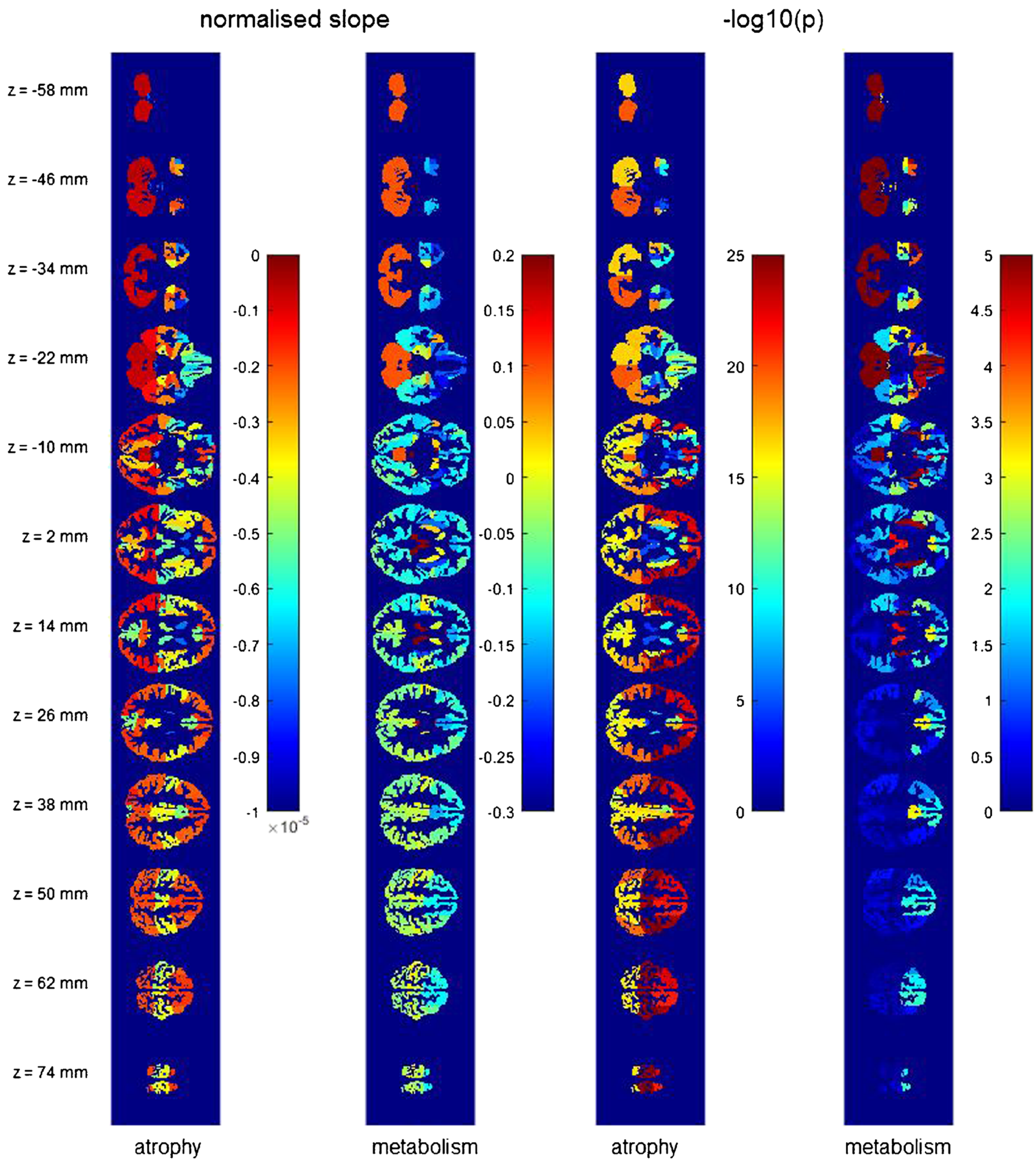

Fig. 6 Comparison between structural atrophy and decrease in brain metabolism with ageing. On the left the slope of the linear regression is give, on the right the corresponding p-value. Atrophy is here quantified as the cube root of the number of voxels within each grey matter region, which should be a good approximation of the cortical thickness. Metabolism is the activity in each brain region after applying the Rousset correction and age-dependent recovery factors. The normalised slope for metabolism is the ΔM value of Eq. 1. The colour scale is truncated for visual purposes

There are some limitations to our study. First we applied a very simple modelling of the PET acquisition, by solely adding Gaussian noise and smoothing. A more realistic modeling of the acquired PET image of the ground truth activity distribution using Monte Carlo simulation would result in more accurate recovery factors. However, we do not expect that this would largely influence the significance of the results, since our method yields a good approximation of the true PET-image. Moreover we assumed an isotropic and uniform resolution of 5mm of the imaging system for both PVE correction techniques. This is an approximation, since the resolution of a PET scanner is not isotropic within the field of view. However, Teo et al. [41] showed that an absolute error of 1mm between the applied PSF and the real PSF leads to a bias of only about 5 %-10 % in recovered activity for the iterative deconvolution. Furthermore, all PET data are expressed as values relative to the uptake in the cerebellum, since no absolute values were available. Normalising to the cerebellum was preferred over the global mean, since several studies have shown that this results in a superior performance, e.g. in the detectability of abnormalities in Alzheimer's or Parkinson's disease [42–45]. This detection is the main purpose of the normal database collected in this study, by comparing the pathological scan to the healthy subjects.

Conclusions

In this study the ability to recover the true activity of two partial volume effect correction methods, the Rousset method and iterative deconvolution, is evaluated using simulated brain phantoms. When a perfect region mask can be obtained, the Rousset method achieves a perfect recovery. For iterative deconvolution, this ability decreases with increasing age, and thus with increasing stages of cortical atrophy. This reveals the need for an age-dependent approach for this PVE correction method in the brain, in this study provided by using age-dependent recovery factors. When applying these techniques to ^{18}F-FDG PET scans of a large healthy subject database, we discovered large regions in the brain with a decreasing metabolism with ageing, especially in the frontal and temporal lobes. An increasing metabolism is found in the cerebellum and thalamus.

Compliance with Ethical Standards

Conflict of interests All authors declare that they have no conflict of interest. All procedures performed in studies involving human participants were in accordance with the ethical standards of the institutional and/or national research committee and with the 1964 Helsinki declaration and its later amendments or comparable ethical standards. Written informed consent was obtained from all individual subjects included in this study according the guidelines of the local medical ethics committee.

References

1. Chételat G, Landeau B, Salmon E, et al. Relationships between brain metabolism decrease in normal aging and changes in structural and functional connectivity. Neuroimage. 2013;76:167–77.
2. Zuendorf G, Kerrouche N, Herholz K, Baron J-C. Efficient principal component analysis for multivariate 3D voxel-based mapping of brain functional imaging data sets as applied to FDG-PET and normal aging. Human Brain Mapping. 2003;18(1):13–21.
3. Moeller JR, Ishikawa T, Dhawan V, et al. The metabolic topography of normal aging. Journal of Cerebral Blood Flow and Metabolism. 1996;16(3):385–98.
4. Petit-Taboué MC, Landeau B, Desson JF, et al. Effects of healthy aging on the regional cerebral metabolic rate of glucose assessed with statistical parametric mapping. Neuroimage. 1998;7(3):176–84.
5. Hsieh T-C, Lin W-Y, Ding H-J, et al. Sex-and Age-Related Differences in Brain FDG Metabolism of Healthy Adults: An SPM Analysis. Journal of Neuroimaging. 2012;22(1):21–7.
6. Willis MW, Ketter TA, Kimbrell TA, et al. Age sex and laterality effects on cerebral glucose metabolism in healthy adults. Psychiatry Research: Neuroimaging. 2002;114(1):23–37.
7. Fujimoto T, Matsumoto T, Fujita S, et al. Changes in glucose metabolism due to aging and gender-related differences in the healthy human brain. Psychiatry Research: Neuroimaging. 2008;164(1):58–72.
8. Yoshizawa H, Gazes Y, Stern Y, et al. Characterizing the normative profile of 18F-FDG PET brain imaging: Sex difference aging effect and cognitive reserve. Psychiatry Research: Neuroimaging. 2014;221(1):78–85.
9. Loessner A, Alavi A, Lewandrowski KU, et al. Regional cerebral function determined by FDG-PET in healthy volunteers: normal patterns and changes with age. Journal of Nuclear Medicine. 1995;36(7):1141–9.
10. Shen X, Liu H, Hu Z, et al. The relationship between cerebral glucose metabolism and age: report of a large brain PET data set. PloS One. 2012;7(12):e51517.
11. Iseki E, Murayama N, Yamamoto R, et al. Construction of a 18F-FDG PET normative database of Japanese healthy elderly subjects and its application to demented and mild cognitive impairment patients. International Journal of Geriatric Psychiatry. 2010;25(4):352–61.
12. Kim I-J, Kim S-J, Kim Y-K. Age-and sex-associated changes in cerebral glucose metabolism in normal healthy subjects: statistical parametric mapping analysis of F-18 fluorodeoxyglucose brain positron emission tomography. Acta Radiologica. 2009;50(10):1169–74.
13. Kochunov P, Mangin J-F, Coyle T, et al. Age-related morphology trends of cortical sulci. Human Brain Mapping. 2005;26(3):210–20.
14. Murphy DGM, DeCarli C, Schapiro MB, et al. Age-related differences in volumes of subcortical nuclei brain matter and cerebrospinal fluid in healthy men as measured with magnetic resonance imaging. Archives of Neurology. 1992;49(8):839–45.
15. Ge Y, Grossman RI, Babb JS, Rabin ML, Mannon LJ, et al. Age-related total gray matter and white matter changes in normal adult brain. Part I: volumetric MR imaging analysis. American Journal of Neuroradiology. 2002;23(8):1327–33.
16. Soret M, Bacharach SL, Buvat I. Partial-volume effect in PET tumor imaging. Journal of Nuclear Medicine. 2007;48(6):932–45.
17. Matsuda H, Ohnishi T, Asada T, et al. Correction for partial-volume effects on brain perfusion SPECT in healthy men. Journal of Nuclear Medicine. 2003;44(8):1243–52.
18. Meltzer CC, Leal JP, Mayberg HS, et al. Correction of PET data for partial volume effects in human cerebral cortex by MR imaging. Journal of Computer Assisted Tomography. 1990;14(4):561–70.
19. Müller-Gärtner HW, Links JM, Prince JL, et al. Measurement of radiotracer concentration in brain gray matter using positron emission tomography: MRI-based correction for partial volume effects. Journal of Cerebral Blood Flow and Metabolism. 1992;12(4):571–83.
20. Quarantelli M, Berkouk K, Prinster A, et al. Integrated software for the analysis of brain PET/SPECT studies with partial-volume-effect correction. Journal of Nuclear Medicine. 2004;45(2):192–201.

21. Park H-J, Lee JD, Chun JW, et al. Cortical surface-based analysis of 18F-FDG PET: measured metabolic abnormalities in schizophrenia are affected by cortical structural abnormalities. Neuroimage. 2006;31(4):1434–44.
22. Curiati PK, Tamashiro-Duran JH, Duran FLS, et al. Age-Related Metabolic Profiles in Cognitively Healthy Elders: Results from a Voxel-Based [18F] Fluorodeoxyglucose–Positron-Emission Tomography Study with Partial Volume Effects Correction. American Journal of Neuroradiology. 2011;32(3):560–5.
23. Ibáñez V, Pietrini P, Furey ML, et al. Resting state brain glucose metabolism is not reduced in normotensive healthy men during aging after correction for brain atrophy. Brain Research Bulletin. 2004;63(2):147–54.
24. Kochunov P, Ramage AE, Lancaster JL, et al. Loss of cerebral white matter structural integrity tracks the gray matter metabolic decline in normal aging. Neuroimage. 2009;45(1):17–28.
25. Kalpouzos G, Chételat G, Baron J-C, et al. Voxel-based mapping of brain gray matter volume and glucose metabolism profiles in normal aging. Neurobiology of Aging. 2009;30(1):112–24.
26. De Leon MJ, Convit A, Wolf OT, et al. Prediction of cognitive decline in normal elderly subjects with 2-[18F] fluoro-2-deoxy-D-glucose/positron-emission tomography (FDG/PET). Proceedings of the National Academy of Sciences. 2001;98(19):10966–71.
27. Yanase D, Matsunari I, Yajima K, et al. Brain FDG PET study of normal aging in Japanese: effect of atrophy correction. European Journal of Nuclear Medicine and Molecular Imaging. 2005;32(7):794–805.
28. Knopman DS, Jack C R, Wiste HJ, et al. 18 F-fluorodeoxyglucose positron emission tomography aging and apolipoprotein E genotype in cognitively normal persons. Neurobiology of Aging. 2014;35(9):2096–106.
29. Nugent S, Tremblay S, Chen KW, et al. Brain glucose and acetoacetate metabolism: a comparison of young and older adults. Neurobiology of Aging. 2014;35(6):1386–95.
30. Nugent S, Castellano C-A, Goffaux P, et al. Glucose hypometabolism is highly localized but lower cortical thickness and brain atrophy are widespread in cognitively normal older adults. American Journal of Physiology-Endocrinology and Metabolism. 2014:ajpendo–00067.
31. Rousset OG, Ma Y, Evans AC. Correction for partial volume effects in PET: principle and validation. Journal of Nuclear Medicine. 1998;39(5):904–11.
32. Thomas BA. Improved brain PET quantification using partial volume correction techniques. 2012. UCL (University College London).
33. Folstein MF, Folstein SE, McHugh PR. Mini-mental state: a practical method for grading the cognitive state of patients for the clinician. Journal of Psychiatric Research. 1975;12(3):189–98.
34. Andreasen NC, O'Leary DS, Cizadlo T, Arndt S, Rezai K, Watkins GL, et al. Remembering the past: two facets of episodic memory explored with positron emission tomography. American Journal of Psychiatry. 1995;152(11):1576–85.
35. Daube-Witherspoon ME, Matej S, Karp JS, Lewitt RM. Application of the row action maximum likelihood algorithm with spherical basis functions to clinical PET imaging. IEEE Transactions on Nuclear Science. 2001;48(1):24–30.
36. Watson CC, Newport DMEC, Casey ME. 1996. Three-dimensional image reconstruction in radiology and nuclear medicine. Springer.
37. Hammers A, Allom R, Koepp MJ, et al. Three-dimensional maximum probability atlas of the human brain with particular reference to the temporal lobe. Human brain mapping. 2003;19(4):224–47.
38. Zaidi H, Ruest T, Schoenahl F, Montandon M-L. Comparative assessment of statistical brain MR image segmentation algorithms and their impact on partial volume correction in PET. Neuroimage. 2006;32(4):1591–607.
39. Hoetjes NJ, van Velden FHP, Hoekstra OS, Hoekstra CJ, Krak NC, Lammertsma AA, et al. Partial volume correction strategies for quantitative FDG PET in oncology. European journal of nuclear medicine and molecular imaging. 2010;37(9):1679–87.
40. Gutierrez D, Montandon M-L, Assal F, Allaoua M, Ratib O, Lövblad K-O, et al. Anatomically guided voxel-based partial volume effect correction in brain PET: impact of MRI segmentation. Computerized Medical Imaging and Graphics. 2012;36(8): 610–9.
41. Teo B-K, Seo Y, Bacharach SL, et al. Partial-volume correction in PET: validation of an iterative postreconstruction method with phantom and patient data. Journal of Nuclear Medicine. 2007;48(5):802–10.
42. Borghammer P, Cumming P, Aanerud J, Gjedde A. Artefactual subcortical hyperperfusion in PET studies normalized to global mean: lessons from Parkinson's disease. Neuroimage. 2009;45(2):249–57.
43. Dukart J, Mueller K, Horstmann A, Vogt B, Frisch S, Barthel H, et al. Differential effects of global and cerebellar normalization on detection and differentiation of dementia in FDG-PET studies. Neuroimage. 2010;49(2):1490–5.
44. Kushner M, Tobin M, Alavi A, Chawluk J, Rosen M, Fazekas F, et al. Cerebellar glucose consumption in normal and pathologic states using fluorine-FDG and PET. Journal of Nuclear Medicine. 1987;28(11):1667–70.
45. Yakushev I, Landvogt C, Buchholz H-G, Fellgiebel A, Hammers A, Scheurich A, et al. Choice of reference area in studies of Alzheimer's disease using positron emission tomography with fluorodeoxyglucose-F18. Psychiatry Research: Neuroimaging. 2008;164(2):143–53.